JMEPEG (2004) 13:653-659
DOI: 10.1361/10599490421547

1059-9495/$19.00

Beta Phase Superplasticity in Titanium Alloys by Boron Modification

Radhakrishna B. Bhat, Seshacharyulu Tamirisakandala, and Daniel B. Miracle

(Submitted August 23, 2004)

Addition of boron to titanium alloys produces fine TiB whiskers in situ with excellent thermal stability and good chemical compatibility with the matrix. These whiskers stabilize a fine-grain microstructure by restricting grain growth at high temperatures in the β phase field. The hot deformation behavior in the β phase field (temperature range 1050-1200 °C) of Ti-6Al-4V alloys modified with two different levels of B additions (1.6 and 2.9 wt.%) produced by powder metallurgy was investigated using hot compression tests in the strain rate range of 10^{-3} to 10^{-1} s^{-1} and hot tensile tests at a nominal strain rate of 6×10^{-4} s^{-1}. The β phase exhibits superplasticity, which occurs due to stabilization of a fine-grain microstructure by the TiB. Matrix grain boundary sliding and β/TiB interface sliding appear to contribute to the β superplasticity. The ability to achieve superplasticity at higher temperatures enable lower flow stresses, improved chemical homogeneity, and high strain rate capability due to enhanced accommodation processes.

Keywords Beta phase, grain pinning, superplasticity, TiB, titanium

1. Introduction

Superplastic forming is a well-established commercial practice for manufacturing aerospace components made of titanium alloys (Ref 1). Several titanium alloys exhibit superplasticity in the α + β phase field, and this process is often combined with diffusion bonding to produce intricate shapes (Ref 2). The superplastic behavior of titanium alloys drastically drops as the temperature approaches the β transus and completely ceases above the β transus due to rapid grain growth in the β phase (Ref 3). Primary deformation processing of titanium alloys is best conducted in the β phase field, which provides the advantages of achieving high levels of deformation in a single step, lower press loads due to the soft nature of body-centered-cubic β, and chemical homogeneity due to enhanced diffusivity. However, rapid grain growth in the β phase field is a serious constraint during β processing of titanium alloys. In this paper, a novel approach to enable superplasticity in the β phase field of titanium alloys via boron modification is presented.

Small additions of boron to titanium alloys produces significant improvements (up to 50%) in specific stiffness and specific strength at room, as well as moderately elevated, temperatures through the formation of fine, dispersed TiB precipitates (Ref 4-9). These precipitates in the boron-modified alloys are whiskers (TiB_w) formed in situ in the titanium matrix, which are distributed uniformly and discontinuously, provide nearly isotropic properties, good workability, and possess reaction-free interfaces. The presence of TiB_w also influences the titanium matrix microstructure at high temperatures, the deformation behavior of the titanium matrix during hot working, and the subsequent microstructural evolution while cooling to room temperature (Ref 8). Borides are known to preferentially segregate to the grain boundaries (Ref 10), and it is possible to stabilize a fine-grained microstructure, which is a prerequisite for enabling conventional structural superplasticity. Structural superplasticity below the β transus has been reported in TiB dispersed Ti-6Al-4V (Ti-64) composites obtained by reaction sintering (Ref 11) and mechanical milling (Ref 12). Transformation superplasticity, while thermal cycling in the temperature range 840-1030 °C, has also been observed in Ti-64/TiB composites (Ref 13, 14). In this work, the deformation behavior of Ti-64 alloys (all compositions are expressed in weight percent), modified with different levels of boron (1.6 and 2.9%) produced by different powder metallurgy techniques, is analyzed above the β transus in the β phase field using hot compression and tension testing. The influence of TiB_w on the matrix deformation mechanism in the β phase field is determined via detailed microstructural examinations.

This paper was presented at the International Symposium on Superplasticity and Superplastic Forming, sponsored by the Manufacturing Critical Sector at the ASM International AeroMat 2004 Conference and Exposition, June 8-9, 2004, in Seattle, WA. The symposium was organized by Daniel G. Sanders, The Boeing Company.

Radhakrishna B. Bhat, UES Inc., 4401 Dayton-Xenia Rd., Dayton, OH 45432; **Seshacharyulu Tamirisakandala,** Department of Mechanical Engineering, Ohio University, Athens, OH 45701; and **Daniel B. Miracle,** Air Force Research Laboratory, Materials and Manufacturing Directorate, Wright-Patterson AFB, OH 45433. Contact e-mail: radha.bhat@fnnet.wpafbml.org.

2. Experimental Methods

2.1 Materials

Ti-64-1.6B was prepared by using the prealloyed (PA) powder metallurgy approach via inert gas atomization, and Ti-64-2.9B was prepared by the blended elemental (BE) approach by blending appropriate amounts of inert gas atomized powders of Ti-64 (average particle size = 30 μm) and titanium (average particle size = 30 μm) with TiB_2 (average particle size = 15 μm) powder in n-butanol using a Turbula mixer for 24 h. The PA Ti-64-1.6B (average powder particle size = 36 μm) or the BE Ti-64-2.9B blend of about 1 kg was packed inside a thick-

Table 1 Chemical compositions of PA Ti-6-4-1.6B and BE Ti-6-4-2.9B

	Composition, wt.%							
Alloy	**Al**	**V**	**B**	**Fe**	**O**	**C**	**N**	**Ti**
PA Ti-6-4-1.6B	6.04	3.97	1.61	0.06	0.18	0.15	0.02	bal
BE Ti-6-4-2.9B	5.53	3.34	2.92	0.06	0.23	0.12	0.02	bal

walled (6.35 mm) can of 70 mm diameter and 130 mm length made of commercial-purity Ti-64, vacuum outgassed at 300 °C for 24 h, and sealed. The can was heated to 1200 °C, soaked for 1 h, and then uniaxially compacted in an extrusion chamber heated to 260 °C using a blind-die. The compact was held at a pressure of 1400 MPa for 180 s and subsequently air cooled to room temperature. The compacted billet of the BE Ti-64-2.9B was then subjected to a heat treatment at 1300 °C for 6 h to ensure completion of the in situ chemical reaction:

$$Ti + TiB_2 \rightarrow 2TiB \quad \text{(Eq 1)}$$

This treatment was not required for the PA Ti-6-4-1.6B compact as the boron in this alloy is already either in the form TiB or in the form of a supersaturated solid solution. The actual overall alloy compositions are Ti-6.2Al-4V-1.6B and Ti-5.5Al-3.5V-2.9B. Complete chemical analysis of both the alloys is provided in Table 1. The nomenclature Ti-6-4-*x*B is chosen to emphasize the fact that even after some of the titanium combines with boron to form TiB, the metal phase composition remains within the specifications (Ref 15) for the commercial alloy Ti-6-4.

2.2 Hot Compression and Tension Testing

Cylindrical specimens of 10 mm diameter and 15 mm height were machined from the compacts via electrodischarge machining (EDM) and the surface was ground to remove the EDM recast layer. Uniaxial compression tests were conducted using a computer-controlled servohydraulic testing machine. An induction coil and susceptor setup was used to heat the specimen and the platens. The specimens were coated with a glass paste (Fiske 604) (Fiske Brothers Refining Company, Toledo, OH) for lubrication and environmental protection. Five concentric grooves of 0.1 mm depth were machined on the top and bottom surfaces for retaining the lubricant during testing. A K-type thermocouple was spot welded to the specimen to monitor and control the temperature of the specimen. Tests were conducted in air in the temperature range 1050-1200 °C at 50 °C intervals. Although boron is not expected to increase the β transus of Ti-6-4 due to very low solid solubility in titanium (<0.1 wt.%) (Ref 10), a slight increase of about 40 °C was observed in PA Ti-6-4-1.6B, which is most likely due to the supersaturation of boron in this rapidly solidified alloy. Nevertheless, the selected test temperature range in both the alloys is above the β transus and corresponds to the full β condition. At each temperature, tests were conducted at predetermined constant true strain rates of 10^{-3}, 10^{-2}, and 10^{-1} s^{-1}. Specimens were deformed to half of their original height in each case and were air cooled to room temperature at a rate of ~20 °C/min. Hot tensile tests were conducted in the same temperature range at an initial strain rate of 6×10^{-4} s^{-1} (constant crosshead speed of 0.02 mm/s) using 2.5 mm thick flat dog-bone shaped specimens of 25.4 mm gage length and 5.6 mm gage width. Specimens were coated with glass lubricant and tested in air, and elongation to failure was recorded.

2.3 Metallography

Hot compressed specimens were bisected along the compression axis, and the cut surface was prepared using standard metallographic polishing techniques. Tensile specimens were polished along the length near the fracture end. Microstructural observations were made using a high-resolution field emission scanning electron microscope (SEM) in the backscatter electron imaging (BEI) mode. Optical microscopy is performed on specimens etched with Kroll's reagent. Microstructural parameter measurements were made using digital image analysis techniques.

3. Results

3.1 Initial Microstructures

The initial microstructures of PA Ti-6-4-1.6B and BE Ti-6-4-2.9B used in the current study are shown in Fig. 1. The microstructure of PA Ti-6-4-1.6B consisted of equiaxed α grains of an average grain size 3 μm with a retained β (due to V addition) volume fraction of about 9% decorating the grain boundaries. The TiB_w comprised 10 ± 1 vol.%, with a 5 μm average length and an aspect ratio of about 10. The TiB_w is uniformly distributed and randomly oriented in the matrix. The microstructural features of BE Ti-6-4-2.9B are essentially similar except that the α grain size and the TiB size are coarser than that of PA Ti-6-4-1.6B by a factor of five. In this alloy, the retained β volume fraction is about 6% and the TiB volume fraction is 18.0 ± 1.4% due to higher concentration of B. A few hollow TiB whiskers are also present.

3.2 Compressive Stress-Strain Curves

Typical true stress-true strain curves of PA Ti-6-4-1.6B and BE Ti-6-4-2.9B in compression at different temperatures and strain rates are shown in Fig. 2(a) and (b), respectively. At all temperatures and strain rates of testing, the flow curves exhibit a peak stress at around 0.02 true plastic strain followed by flow softening and apparent steady-state behavior. Typical flow curves in tension for BE Ti-6-4-2.9B at an initial strain rate of 6×10^{-4} s^{-1} and different temperatures are shown in Fig. 2(c). The decrease in flow stress during tensile deformation is most likely due to the reduced strain rate (under constant crosshead speed) as well as rotation of grains and TiB_w to orientations that facilitate easy plastic flow. These features are similar in PA Ti-6-4-1.6B. The strain rate sensitivity (m) values were calculated using:

$$m = \frac{\partial \log \sigma}{\partial \log \dot{\varepsilon}} \quad \text{(Eq 2)}$$

and are given in Table 2. In the case of PA Ti-6-4-1.6B, m is around 0.3 at all temperatures and strain rates $\leq 10^{-2}$ s^{-1}, whereas for BE Ti-6-4-2.9B, a high value of m is exhibited at

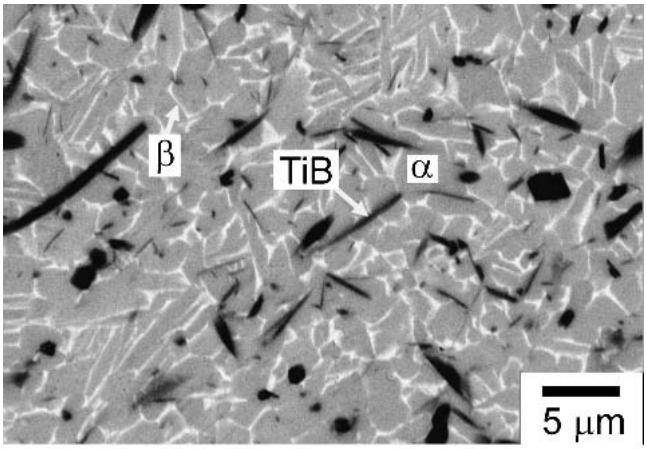

(a)

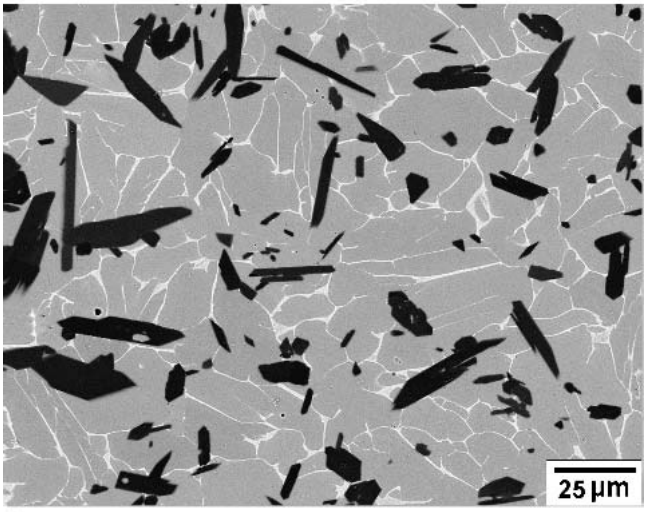

(b)

Fig. 1 Backscatter electron images of starting microstructures of (a) PA Ti-6-4-1.6B and (b) BE Ti-6-4-2.9B. The gray background is the α matrix, the bright phase is β, and the dark phase is TiB.

the highest temperature and lowest strain rate of testing. In both alloys, the *m* values increase with decreasing strain rate.

3.3 Tensile Behavior

Elongations-to-failure obtained at different temperatures and an initial strain rate of 6×10^{-4} s^{-1} are shown in Fig. 3. Within the tested conditions, the peak tensile elongation is above 250% for PA Ti-6-4-1.6B and above 150% for BE Ti-6-4-2.9B in the β phase field. In the case of PA Ti-6-4-1.6B, the tensile ductility exhibits a peak at 1150 °C followed by rapid drop, whereas in BE Ti-6-4-2.9B, a steady increase is observed with increasing temperature. Figure 4 shows tensile specimens at peak ductility conditions that exhibit diffused and multiple necking near the fracture region. The microstructures in the grip and gage portion of a PA Ti-6-4-1.6B tensile specimen deformed at 1150 °C are shown in Fig. 4(a) and (b), respectively. To verify whether the α grain size in this microstructure represents the prior β grain size, static heat treatments were performed at different temperatures in the β phase field and the samples were rapidly quenched using brine solution (NaCl + water) to capture the structure at high temperature. The microstructure of the BE Ti-6-4-2.9B sample quenched from 1200 °C is shown in Fig. 5. The microstructure consists of martensite needles in prior β grains of about 15 μm, which is similar to the starting grain size (Fig. 1b). The microstructure in the gage portion of BE Ti-6-4-2.9B specimen after tensile testing at 1200 °C is shown in Fig. 6, while Fig. 7(a) and (b) show the microstructures in the grip and gage portions of the Ti-6-4-1.6B tensile specimen tested at 1200 °C.

4. Discussion

4.1 Initial Microstructure

The microstructure (Fig. 1) of boron modified Ti-6-4 alloys is sensitive to, and dependent on, the prior processing history. The PA approach involves rapid solidification of the boron containing alloy melt, which results in very fine TiB and matrix grain size compared with the BE method. The PA approach also results in a supersaturated solid solution of boron in titanium, which is forced out in the form of fine in situ TiB whiskers during subsequent thermal exposure in the solid state (Ref 16). The BE approach involves a high-temperature heat treatment to convert TiB_2 to TiB, and this results in a relatively coarser matrix grain size as compared with the PA material. In addition, the morphology and size of the TiB produced in the BE method is a function of both the number of available nuclei (related to the TiB_2 particle size) and the time and temperature at which conversion reaction was conducted. The TiB produced in the BE approach is about five times coarser compared with that of PA approach, and the morphology is typically platelike compared with the whisker morphology in the PA alloy. In either case, the matrix microstructure obtained in boron-modified Ti-6-4 alloys is equiaxed α in contrast to the lamellar (i.e., transformed β) colony structure expected in Ti-6-4 upon slow cooling from the β phase (Ref 15). The microstructures in Fig. 1(a) and (b) clearly show that the presence of TiB_w significantly influences the $\beta \rightarrow \alpha$ phase transformation and causes a change in the morphology of the α-phase nucleating from the β phase while cooling across the β transus. This observation is in agreement with the findings reported by Banerjee et al. (Ref 17) on Ti-6-4-2B produced by laser engineered net-shape processing.

4.2 β-phase Superplasticity

The prerequisites for conventional superplasticity are: (a) a fine-grained starting microstructure (grain size < 10-15 μm), (b) a deformation temperature exceeding 0.4 T_m where T_m is the absolute melting temperature, and (c) a specific range of strain rates (usually 10^{-4} to 10^{-1} s^{-1}) (Ref 18). The features of superplastic deformation include: (a) low-flow stress values independent of strain, (b) *m* values exceeding 0.3, (c) large tensile elongations-to-failure (usually >200%), (d) diffused/multiple necking in the tensile samples, and (e) retention of the equiaxed microstructure after deformation. All these features have been observed in the boron-modified Ti-6-4 alloys and therefore confirm the occurrence of superplasticity in the β phase.

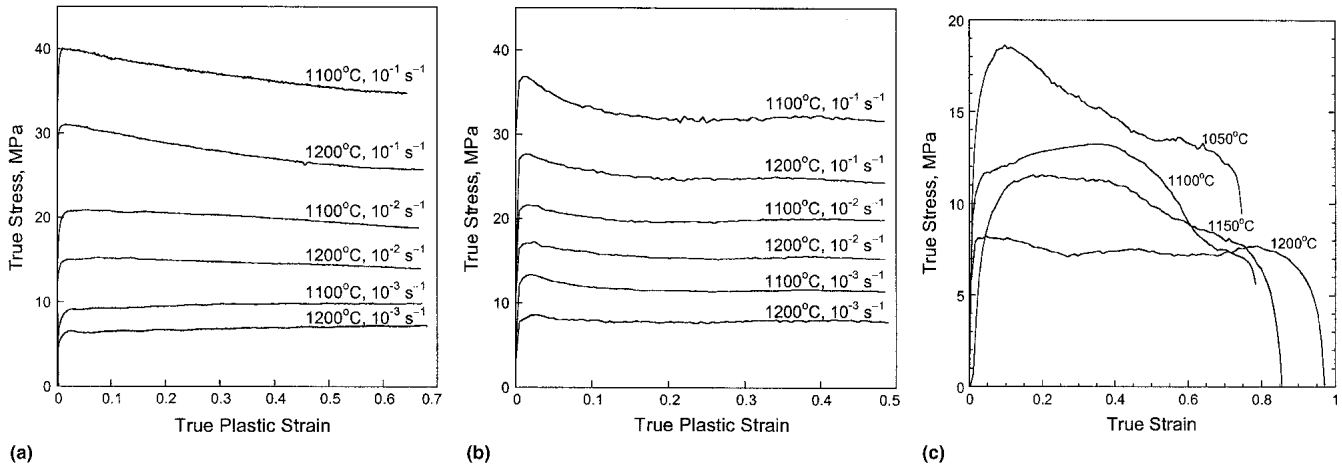

Fig. 2 Flow curves in the β phase field and different strain rates under compression for (a) PA Ti-6-4-1.6B, (b) BE Ti-6-4-2.9B, and (c) under tension for BE Ti-6-4-2.9B at an initial strain rate of 6×10^{-4} s^{-1}

Table 2 Strain rate sensitivity values as a function of temperature and strain rate

Material	Strain rate, s^{-1}	Temperature 1050 °C	1100 °C	1150 °C	1200 °C
PA Ti-6-4-1.6B	10^{-3}	0.37	0.35	0.33	0.32
	10^{-2}	0.29	0.28	0.28	0.30
	10^{-1}	0.23	0.23	0.24	0.24
BE Ti-6-4-2.9B	10^{-3}	0.23	0.22	0.23	0.31
	10^{-2}	0.20	0.21	0.23	0.23
	10^{-1}	0.20	0.21	0.21	0.20

In conventional superplasticity, one of the dominant features is the role played by grain boundary sliding (GBS), which is not expected to occur in the β phase of boron-free Ti-6-4 due to extensive grain growth. However, the presence of TiB arrests the grain growth and stabilizes a fine-grained microstructure, enabling superplasticity in the β phase field. There are two significant features to be noted in the microstructure of the tensile tested specimen (Fig. 4a). First, the matrix microstructure remains primarily equiaxed α + β even after deformation processing in the β phase field. Second, the α grain size is essentially unchanged compared with the grain size of the starting material even after processing high in the β phase field. The static heat treatment experiment confirmed that the α grain boundaries in the air-cooled microstructure indeed represent the prior β grain boundaries (Fig. 5, 6). The absence of β grain growth indicates that TiB_w effectively pins the grain boundaries. Borides in titanium alloys have been typically observed to segregate to the grain boundaries and inhibit grain growth by the well-known Zener pinning mechanism (Ref 19). A stabilized fine β grain size due to the presence of TiB_w enables superplasticity in the boron-modified Ti-6-4. As for the TiB_w, while they were randomly oriented in the undeformed condition (Fig. 4a), the majority of the TiB are aligned along the tensile axis (Fig. 4b and 6), which indicates significant rigid body rotation of the TiB whiskers in a plastically deforming matrix. Schuh and Dunand (Ref 14) have discussed this phenomenon in detail with reference to transformation superplasticity in a similar material.

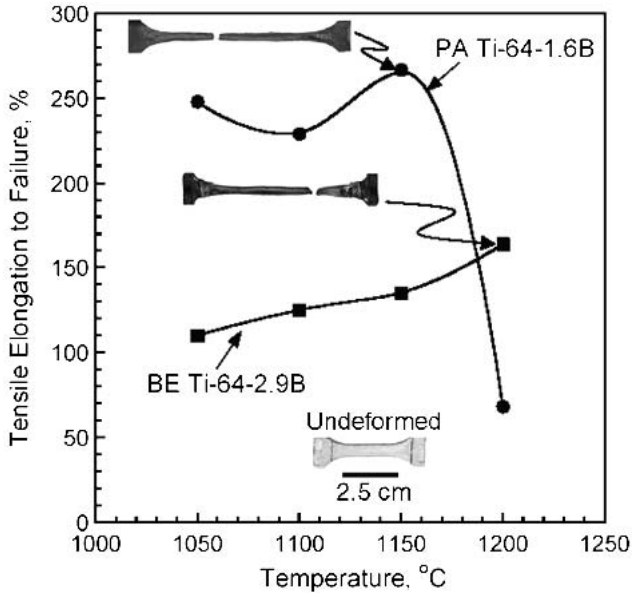

Fig. 3 Variation of tensile ductility with temperature for PA Ti-6-4-1.6B and BE Ti-6-4-2.9B at an initial strain rate of 6×10^{-4} s^{-1}

Although the phase transformation occurring in titanium while cooling to room temperature makes it impossible to retain the dynamic microstructural features, insights on the deformation mechanism can be obtained from the features of voids that form during superplastic deformation at high strains. In the microstructure from the gage portion of the Ti-6-4-2.9B tensile test specimen (Fig. 6), cavitation is observed at the grain boundaries and triple junctions. Similar features were observed in PA Ti-6-4-1.6B. The indirect evidence of retention of the original grain size and morphology and the formation of voids at the grain boundaries indeed demonstrate that GBS predominantly occurs during superplastic deformation in the β phase field. Cavities are also found at the matrix/TiB interface and

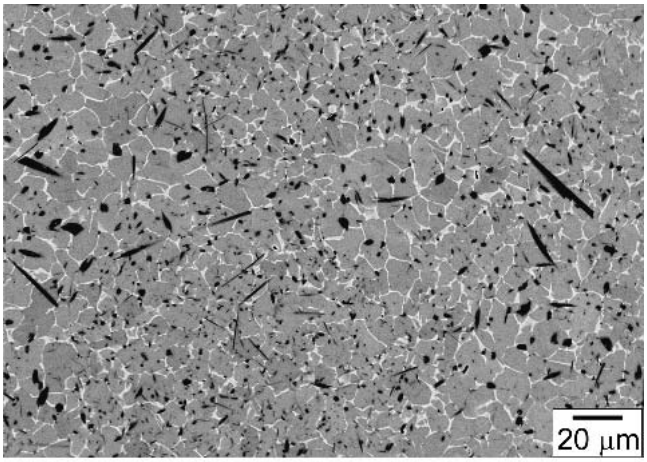

(a)

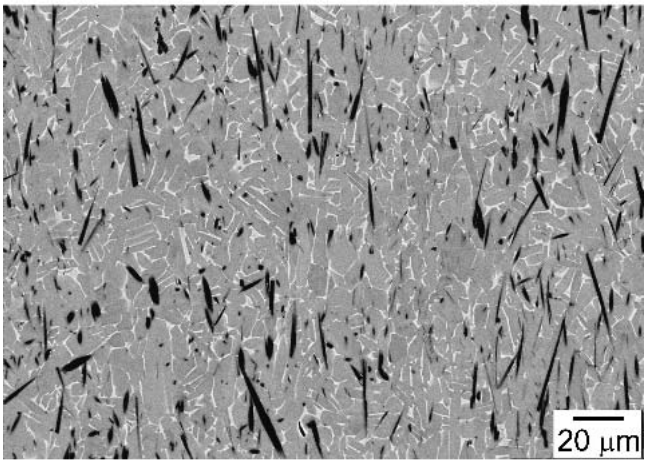

(b)

Fig. 4 Backscatter electron images of PA Ti-6-4-1.6B tensile specimen after testing at 1150 °C. (a) Grip. (b) Gage

whisker ends (Fig. 6), which are indicative of the occurrence of interfacial sliding during β superplasticity. Cavitation at the grain boundaries and interfaces are reduced with an increase in temperature, which is due to reduced stress concentrations and increased diffusivity. The overall elongations are lower for the BE Ti-6-4-2.9B compared with PA Ti-6-4-1.6B at the same strain rate (Fig. 3). This can be attributed to the relatively coarser starting grain size (Fig. 1) and higher volume fraction of coarser TiB, which produce larger stress concentrations at the interfaces. The rapid drop in elongation at 1200 °C in PA Ti-6-4-1.6B can be attributed to abnormal grain growth in this alloy at this temperature as can be seen from Fig. 7. The average grain size in the grip portion (undeformed region, Fig. 7a) is about 14 μm, while it is about 20 μm in the gage portion (deformed region, Fig. 7b). Grain growth by a factor of five combined with dynamic grain growth occurring at these temperatures reduces the superplastic response of this alloy. Comparison of these microstructures with that of BE Ti-6-4-2.9B (Fig. 6) reveals that grain growth is significant in the case of the lower volume fraction TiB alloy. An enhanced oxidation rate with an increase in temperature also causes embrittlement

Fig. 5 Optical micrograph of BE Ti-6-4-2.9B heat treated at 1200 °C for 30 min followed by rapid water quench (etched with Kroll's reagent)

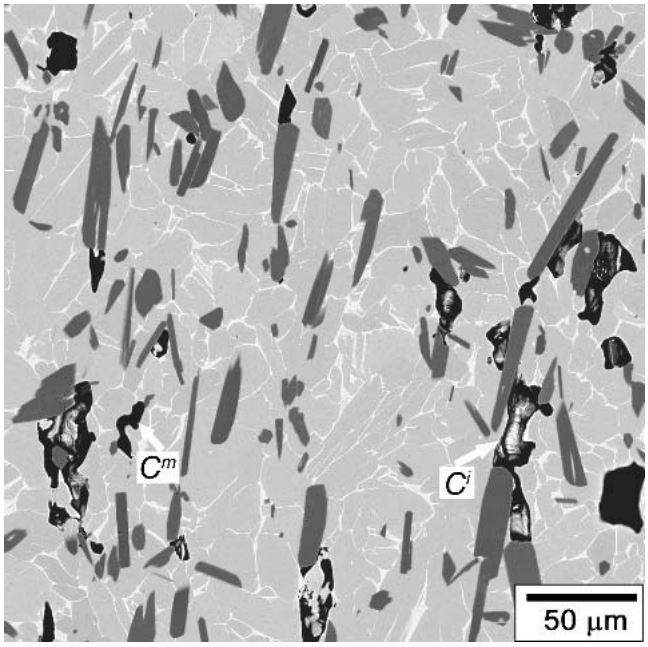

Fig. 6 Backscatter electron image of BE Ti-6-4-2.9B tensile specimen tested at 1200 °C. The tensile axis is vertical. Filled arrows indicate cavitation at grain boundaries and triple junction, and open arrows indicate cavitation at matrix/TiB interfaces.

of grain boundaries leading to a reduction in superplastic response.

5. Industrial Feasibility of β Phase Superplasticity

To demonstrate the industrial feasibility of β phase superplasticity in boron-modified Ti-6-4, a forging experiment was performed using a vacuum hot press. A PA Ti-6-4-1.6B compact was prepared by the same process described previously and a preform of 33 mm diameter and 60 mm height was machined via EDM from the compact. This preform and the

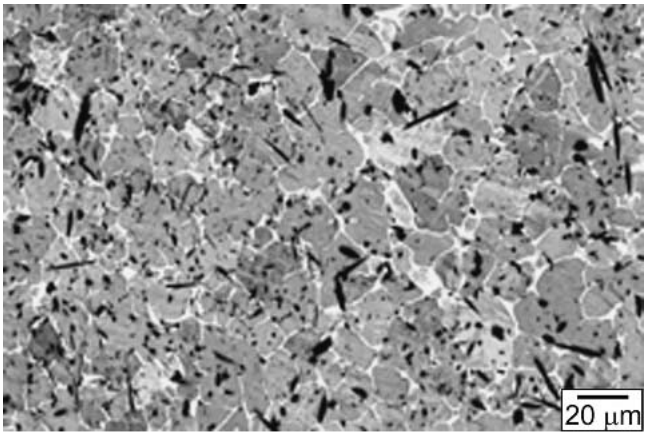

(a)

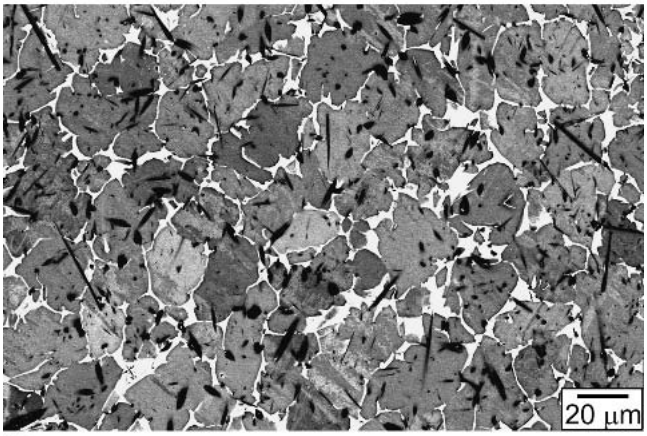

(b)

Fig. 7 Backscatter electron images of PA Ti-6-4-1.6B tensile specimen tested at 1200 °C in the (a) grip and (b) gage portion. The tensile axis is vertical.

graphite die setup used to isothermally forge this preform under superplastic conditions (1150 °C and 10^{-3} s^{-1}) is shown in Fig. 8(a). The forged larger disk of 10 mm height and 75 mm diameter is shown in Fig. 8(b). Figure 8(c) shows the SEM BSE micrograph of the radial section of this disc, indicating that the equiaxed α microstructure is maintained and grain growth is restricted during the β phase forging. A smaller disk forged under similar conditions using a different die set (not shown here) is also shown in Fig. 8(b). The successful use of low-cost and easily machinable graphite dies indicates that the flow stresses are sufficiently low enough in the β phase field (a characteristic of the superplasticity process). This feature enables the use of low-capacity presses for net-shape component manufacture. The clear reproduction of AFRL on the forged disc (Fig. 8b) indicates that β superplastic forging process is capable of reproducing fine details.

The ability to restrict grain growth and achieve superplasticity in the β phase field of titanium alloys has several advantages. In general, the formability of titanium alloys is better with an increased amount of softer β phase. This aspect is advantageously used in thermohydrogen processing, wherein the addition of hydrogen to titanium lowers the β transus and,

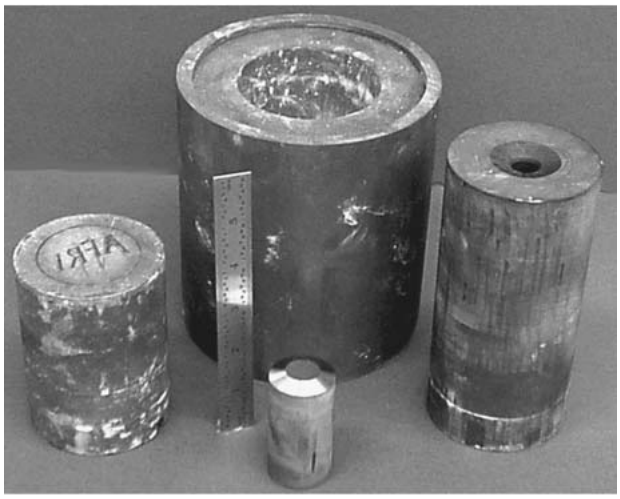

(a)

(b)

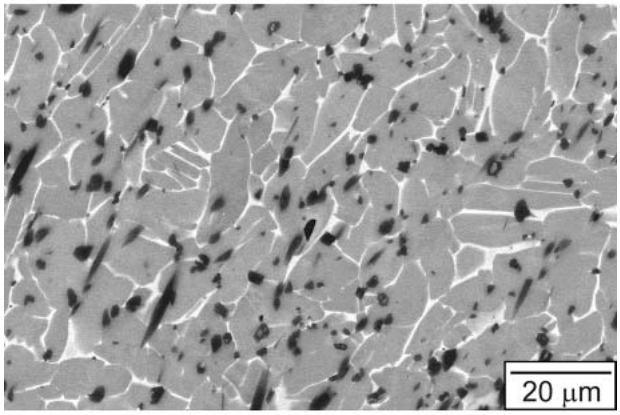

(c)

Fig. 8 Superplastic forging of PA Ti-6-4-1.6B at 1150 °C and 10^{-3} s^{-1}. (a) Graphite dies setups. (b) Forged disks. (c) Backscatter electron image in the radial section of larger disc

in turn, increases the proportion of the β phase at a given temperature in the α + β region (Ref 20). In this work, β phase processing is enabled by restricting grain growth and attaining

microstructural stability above the β transus. The superplastic response of the material in the β phase is an added advantage. The ability to form superplastically at higher temperatures, that is, in the β phase field, reduces the material flow stress significantly, which can be advantageously used to perform normal forming operations using moderate-capacity presses and low-cost dies. Processing in the β phase field also improves the chemical homogeneity due to enhanced diffusion rates. In addition, the well-established advantages of superplastic forming, including uniform metal flow, near-net/net-shape forming (reduced machining), no resultant residual stresses, and no springback, would make β superplastic forming more attractive. Although superplasticity in titanium alloys is an established commercial practice, its use is restricted to aerospace components primarily due to slow strain rates (10^{-4} to 10^{-3} s^{-1}) and the high cost associated with conventional superplasticity. The β superplasticity, on the other hand, occurs at two orders of magnitude higher strain rates than the conventional practices, thereby reducing the processing times significantly and improving the affordability of component manufacturing. At room temperature, boron-modified titanium alloys exhibit significant enhancements in stiffness and strength at the expense of ductility (Ref 9). However, optimization of thermomechanical processing parameters and alloy composition is likely to provide a good combination of properties for a wide variety of applications.

6. Conclusions

- Addition of boron to conventional titanium alloys such as Ti-6-4 produces fine TiB whiskers that restrict grain growth in the β phase field and stabilize a fine-grained microstructure, thereby enabling deformation processing in the β phase field.
- Boron-modified titanium alloys also exhibit superplasticity in the β phase field.
- Microstructural evidence reveals grain boundary as well as matrix/TiB interface sliding during β superplastic deformation.
- Superplastic deformation at high-temperatures allows titanium alloys to be shape formed at strain rates two orders of magnitude higher than the conventional low-temperature superplasticity, which can be advantageously used to improve the affordability of component manufacture.

Acknowledgment

This work was conducted as part of in-house research effort of the Metallic Composites research group of the Materials and Manufacturing Directorate, Air Force Research Laboratory. Two of the authors (R.B.B. and S.T.) were supported under the auspices of Air Force Contract No. F33615-01-C-5214 and F33615-99-C-5803.

References

1. D.G. Sanders, The History and Current State-of-the-Art in Air Frame Manufacturing Using Superplastic Forming Technologies, *Advances in Superplasticity and Superplastic Forming,* E.M. Taleff, P.A. Friedman, P.A. Krajewski, R.S. Mishra, and J.G. Schroh, Ed., TMS, 2004
2. W. Beck, Superplastic Forming and Diffusion Bonding of Titanium and Titanium Alloys, *Titanium and Titanium Alloys,* C. Leyens and M. Peters, Ed., Wiley-VCH Verlag GmbH & Co. KGaA, Weinheim, Germany, 2003, p 273-288
3. M.W. Mahoney, Superplastic Forming of Titanium Alloys, *Materials Properties Handbook, Titanium Alloys,* R. Boyer, G. Welsch, and E.W. Collings, Ed., ASM International, 1994, p 1101
4. T. Godfrey, P.S. Goodwin, and C.M. Ward-Close, Titanium Particulate Metal Matrix Composites Reinforcement, Methods, and Mechanical Properties, *Adv. Eng. Mater.,* Vol 2, 2000, p 85-92
5. T. Saito, The Automotive Application of Discontinuously Reinforced TiB-Ti Composites, *J. Met.* Vol 56 (No. 5), 2004, p 33-36
6. S. Abkovitz, S.M. Abkovitz, H. Fisher, and P.J. Schwartz, CermeTi® Discontinuously Reinforced Ti-Matrix Composites, Manufacturing, Properties, and Applications, *J. Met.* Vol 56 (No. 5), 2004, p 37-41
7. C.F. Yolton, The Pre-Alloyed Powder Metallurgy of Titanium with Boron and Carbon Additions, *J. Met.* Vol 56 (No. 5), 2004, p 56-59
8. S. Tamirisakandala, R.B. Bhat, V.A. Ravi, and D.B. Miracle, Powder Metallurgy Ti-6Al-4V-xB Alloys, Processing, Microstructure, and Properties, *J. Met.* Vol 56 (No. 5), 2004, p 60-63
9. S. Gorsse and D.B. Miracle, Mechanical Properties of Ti-6Al-4V/TiB Composites with Randomly Oriented and Aligned TiB Reinforcements, *Acta Mater.,* Vol 51, 2003, p 2427-2442
10. J. Murray, Ed., *Phase Diagrams of Binary Titanium Alloys,* ASM International, 1987, p 33
11. M. Kobayashi, K. Funami, S. Suzuki, and C. Ouchi, Manufacturing Process and Mechanical Properties of Fine TiB Dispersed Ti-6Al-4V Alloy Composites Obtained by Reaction Sintering, *Mater. Sci. Eng.,* Vol A243, 1998, p 279-284
12. T.M.T. Godfrey, A. Wisbey, A. Brown, R. Brydson, and C. Hammond, Superplasticity and Production of Mechanically Milled Ti-6Al-4V-0.5B, *Mater. Sci. Technol.,* Vol 16, 2000, p 1302-1308
13. C. Schuh and D.C. Dunand, Load Transfer During Transformation Superplasticity of Ti-6Al-4V/TiB Whisker-Reinforced Composites, *Scr. Mater.,* Vol 45 (No. 6), 2001, p 631-638
14. C. Schuh and D.C. Dunand, Whisker Alignment of Ti-6Al-4V/TiB Composites during Deformation by Transformation Superplasticity, *Int. J. Plast.* Vol 17 (No. 3), 2001, p 317-340
15. R. Boyer, G. Welsch, and E.W. Collings, Ed., *Material Properties Handbook, Titanium Alloys,* ASM International, 1994, p 483-636
16. Z. Fan, L. Chandrasekaran, C.M. Ward-Close, and A.P. Miodownik, The Effect of Pre-consolidation Heat Treatment on TiB Morphology and Mechanical Properties of Rapidly Solidified Ti-6Al-4V-xB alloys, *Scr. Metall.,* Vol 32 (No. 6), 1995, p 833-838
17. R. Banerjee, P.C. Collins, A. Genc, and H.L. Fraser, Direct Laser Deposition of In-Situ Ti-6Al-4V-TiB Composites, *Mater. Sci. Eng.,* Vol A358, 2003, p 343-349
18. O.A. Kaibyshev, *Superplasticity of Alloys, Intermetallides and Ceramics,* Springer-Verlag, 1992, p 4
19. J.A. Christodoulou and H.M. Flower, The Role of Borides in Near-γ Titanium Aluminides, *Adv. Eng. Mater.,* Vol 2 (No. 10), 2000, p 631-638
20. O. Senkov and F.H. Froes, Thermohydrogen Processing of Titanium alloys, *Int. J. Hydrogen Energy,* Vol 24, 1999, p 565-576